

Comparison of Methods for Characterizing Nonideal Solute Self-Association by Sedimentation Equilibrium

David J. Scott^{†*} and Donald J. Winzor[‡]

[†]National Center for Macromolecular Hydrodynamics, University of Nottingham School of Biosciences, Sutton Bonington, United Kingdom; and [‡]School of Chemistry and Molecular Biosciences, University of Queensland, Brisbane, Queensland, Australia

ABSTRACT We have examined in detail analytical solutions of expressions for sedimentation equilibrium in the analytical ultracentrifuge to describe self-association under nonideal conditions. We find that those containing the radial dependence of total solute concentration that incorporate the Adams-Fujita assumption for composition-dependence of activity coefficients reveal potential shortcomings for characterizing such systems. Similar deficiencies are shown in the use of the NONLIN software incorporating the same assumption about the interrelationship between activity coefficients for monomer and polymer species. These difficulties can be overcome by iterative analyses incorporating expressions for the composition-dependence of activity coefficients predicted by excluded volume considerations. A recommendation is therefore made for the replacement of current software packages by programs that incorporate rigorous statistical-mechanical allowance for thermodynamic nonideality in sedimentation equilibrium distributions reflecting solute self-association.

INTRODUCTION

Over fifty years ago, Adams and Fujita (1) proposed a readily usable and mathematically expedient solution for the analysis of sedimentation equilibrium distributions where self-association occurs under thermodynamically nonideal conditions. This was achieved by invoking an assumption that the activity coefficients of the different oligomeric forms of a protein can be described in terms of total weight-concentration of protein (\bar{c}) by the relationship

$$\ln \gamma_i = iBM_A\bar{c}, \quad (1)$$

where M_A is the molecular mass of monomer, γ_i is the activity coefficient of the polymer comprising i monomers, and B is an empirical constant to be evaluated from the analysis. However, the description of thermodynamic nonideality in terms of Eq. 1 was shown by statistical-mechanical reasoning to be invalid theoretically for proteins because of the consequent requirement that a concentration-dependent variable (BM_A) be obtained as a curve-fitting parameter (2). More rigorous procedures for the characterization of protein self-association have therefore been developed over the past three decades to allow for the effects of thermodynamic nonideality on the statistical-mechanical basis of excluded volume (3–7) and scaled particle theory (8–11).

Unfortunately, the Adams-Fujita assumption has been incorporated into the NONLIN computer software (12) that was developed to accommodate a growing realization (13) that direct analysis affords the best means of extracting equilibrium constants from sedimentation equilibrium distributions for self-associating solutes. Furthermore, the Beckman Origin software package (14) and the published INVEQ

algorithm (15) incorporate the same theoretical expediency. In view of the heavy reliance placed on software for the extraction of association constants from sedimentation equilibrium distributions, it is important to examine more closely the effect of the Adams-Fujita assumption (1) on the reliability of the resultant quantitative characterization of protein self-association. The major purpose of this article is to present the relevant thermodynamic theory that 1), highlights theoretical shortcomings of the current software packages for characterizing protein self-association by sedimentation equilibrium; and 2), provides potential avenues for their replacement by more rigorous procedures.

THEORETICAL CONSIDERATIONS

Initial attempts to characterize nonideal solute self-association directly from the form of the sedimentation equilibrium distribution by analysis (3,4) or by simulation (12) were necessarily iterative because of the arbitrary separation of self-association and thermodynamic nonideality effects. In fact a simpler, and thermodynamically more rigorous, approach to the problem of making allowance for the effects of thermodynamic nonideality on protein self-association had already been suggested by Hill and Chen (16), but two decades elapsed before advantage was taken (5) of that important but overlooked publication.

Self-association as a form of thermodynamic nonideality

The theoretical breakthrough was the stance taken by Hill and Chen (16) that a self-associating solute is a single thermodynamic component, whereupon the effects of self-association should be regarded as part of the virial coefficients describing nonideality in terms of the total base-molar

Submitted March 4, 2009, and accepted for publication May 19, 2009.

*Correspondence: dj.scott@nottingham.ac.uk

Editor: Kathleen B. Hall.

© 2009 by the Biophysical Society
0006-3495/09/08/0886/11 \$2.00

doi: 10.1016/j.bpj.2009.05.028

concentration of solute ($\bar{C} = \bar{c}/M_A$), where M_A is the monomer molar mass. Adoption of that viewpoint leads to the following expression for the molar thermodynamic activity of monomer (z_A) as a series expansion in \bar{C} ,

$$z_A = \bar{C} \exp \left[2B_2 \bar{C} + \frac{3}{2} B_3 \bar{C}^2 + \dots \right], \quad (2)$$

which is formally identical with that for a nonassociating solute except that the second and third virial coefficients (B_2, B_3) contain additional terms to accommodate solute self-association. For a reversibly dimerizing system ($2A \rightleftharpoons P$) the two virial coefficients are

$$B_2 = B_{AA} - K_2, \quad (3a)$$

$$B_3 = B_{AAA} - 8K_2 B_{AA} + 2K_2 B_{AP} + 4K_2^2, \quad (3b)$$

of chemical reactions is more logically expressed in molar terms, there is still clearly a preference within the ultracentrifuge field for the measurement of equilibrium constants on a weight-concentration scale. For the conversion of Eq. 5 to such a basis we note that $B_2 = 2B_{AA}/M_A^2$ and $X_2 = 2K_2/M_A$, where the units of the experimental coefficient (B_2) are $L \text{ mol g}^{-2}$, and where X_2 expresses the dimerization constant ($L \text{ g}^{-1}$) on a weight-concentration basis. In these terms Eq. 5 becomes

$$\frac{M_A(1 - \bar{v}\rho_s)\omega^2}{2RT}(r^2 - r_F^2) = -\ln(M_A z_A(r_F)) + \ln \bar{c}(r) + (B_2 M_A - X_2)\bar{c}(r) + \dots \quad (6a)$$

or, in logarithmic format (7)

$$(r^2 - r_F^2) = \frac{2RT(-\ln(M_A z_A(r_F)) + \ln \bar{c}(r) + (B_2 M_A - X_2)\bar{c}(r) + \dots)}{M_A(1 - \bar{v}\rho_s)\omega^2}. \quad (6b)$$

where $K_2 = z_P/z_A^2$ is the molar equilibrium constant for dimer formation. B_{AA} and B_{AAA} are the second and third virial coefficients for nonassociative interaction between two and three monomers, respectively, whereas B_{AP} is the corresponding notional second virial coefficient for nonassociative interaction between monomer and dimer. In principle, the characterization of nonideal self-association becomes a relatively simple problem when the thermodynamic activity of monomer (z_A) can be monitored as a function of total solute concentration (\bar{C}). Sedimentation equilibrium provides that information (5,13,17,18).

In an experiment conducted at angular velocity ω and absolute temperature T , the radial distribution of monomer (with molar mass M_A) is described by the expression (13,19)

$$z_A(r) = z_A(r_F) \exp \left[\frac{M_A(1 - \bar{v}\rho_s)\omega^2}{2RT}(r^2 - r_F^2) \right] \quad (4)$$

as the relationship between the thermodynamic activity of monomer, $z_A(r)$, at radial distance r to its value, $z_A(r_F)$, at some fixed reference radial position r_F . \bar{v} is the partial specific volume of monomer, ρ_s the solvent density (17,20), and R the universal gas constant. Replacement of z_A in Eq. 2b by this expression then leads to the relationship (5)

$$\frac{M_A(1 - \bar{v}\rho_s)\omega^2}{2RT}(r^2 - r_F^2) = -\ln z_A(r_F) + \ln \bar{C}(r) + 2(B_{AA} - K_2)\bar{C}(r) + \dots, \quad (5)$$

where the truncation conforms with the usual experimental practice of restricting nonideality considerations to the quadratic power of concentration. Although the description

This expression provides a tractable means of characterizing solute dimerization by nonlinear regression analysis of $[(r^2 - r_F^2), \bar{C}(r)]$ data sets to obtain $\ln [M_A z_A(r_F)]$ and $(B_2 M_A - X_2)$ as the two curve-fitting parameters. Evaluation of the dimerization constant is clearly conditional upon the assignment of a magnitude to $B_2 M_A$. In that regard, an approximate value of the corresponding molar second virial coefficient (B_{AA}) is usually obtained (17,18,21) as

$$B_{AA} = \frac{4\pi L R_A^3}{3} + \frac{Z_A^2(1 + 2\kappa R_A)}{4I(1 + \kappa R_A)^2}, \quad (7)$$

where R_A is the radius of a spherical monomer with net charge Z_A spread uniformly over its surface; and where κ , the inverse screening length (cm^{-1}), is deduced from the ionic strength I as $3.27 \times 10^7 \sqrt{I}$. Avogadro's number (L) converts the second virial coefficient from a molecular to a molar basis.

However, the application of Eq. 6 is restricted to the characterization of relatively weak solute dimerization because of systematically slower convergence of the series in the exponent of Eq. 2 with increasing values of X_2 (7,21). To amplify that statement we consider the contributions made by the linear and quadratic concentration terms in the expression

$$\ln \left(\frac{z_A}{\bar{C}} \right) = 2(B_{AA} - K_2)\bar{C} + \frac{3}{2}(4K_2^2 - 2K_2(4B_{AA} - B_{AP}) + B_{AAA})\bar{C}^2 + \dots, \quad (8)$$

which is obtained by incorporating Eqs. 3a and 3b into the logarithmic form of Eq. 2. Dependencies of those two contributions upon the magnitude assigned to the dimerization constant were calculated on the basis that $B_{AA} = 450 \text{ L mol}^{-1}$,

$B_{AP} = 1300 \text{ L mol}^{-1}$, and $B_{AAA} = 127,300 \text{ L}^2 \text{ mol}^{-2}$, values calculated previously for an uncharged monomer-dimer system with $R_A = 3.55 \text{ nm}$ and a dimer radius of 4.47 nm (7). For illustrative purposes the base-molar solute concentration \bar{C} has been taken as 0.1 mM , or 7 g/L for the 70 kDa monomer under previous consideration (7). From Fig. 1 it is evident that the contribution of the quadratic term (\square) is of negligible magnitude for small values of K_2 . However, for dimerization constants $> 2B_{AA}$ (900 L/mol), the quadratic term contributes significantly to the magnitude of $\ln(z_A/\bar{C})$. Furthermore, for $K_2 > 6B_{AA}$, the contribution of the quadratic term exceeds that of its linear counterpart (\blacksquare), a situation which signifies divergence of the series. Therein lies the reason for the modification of Eq. 6 by adding a quadratic concentration term to improve the reliability of the dimerization constant deduced from the magnitude of the linear concentration coefficient that emanates from nonlinear least-squares curve-fitting to Eq. 6 (7). Nevertheless, valid application of this approach is still restricted to studies of weak solute self-association.

Fortunately, that limitation can be overcome by using the inverse relationship wherein \bar{c} is expanded as a series in monomer activity, the relevant expression for the analysis of sedimentation equilibrium distributions being (5)

$$\begin{aligned} \bar{c}(r) = & M_A z_A(r_F) \psi_A(r) + (X_2 - B_2 M_A) \\ & \times [M_A z_A(r_F) \psi_A(r)]^2 + P [M_A z_A(r_F) \psi_A(r)]^3 + \dots, \end{aligned} \quad (9a)$$

where

$$\psi_A(r) = \exp\left(M_A(1 - \bar{v}\rho_s)\frac{\omega^2}{2RT}(r^2 - r_F^2)\right). \quad (9b)$$

Estimates of $M_A z_A(r_F)$ and $(X_2 - B_2 M_A)$ can thus be obtained as two curve-fitting parameters emanating from nonlinear regression analysis of $[\psi_A(r), \bar{c}(r)]$ data in terms of Eq. 9a,

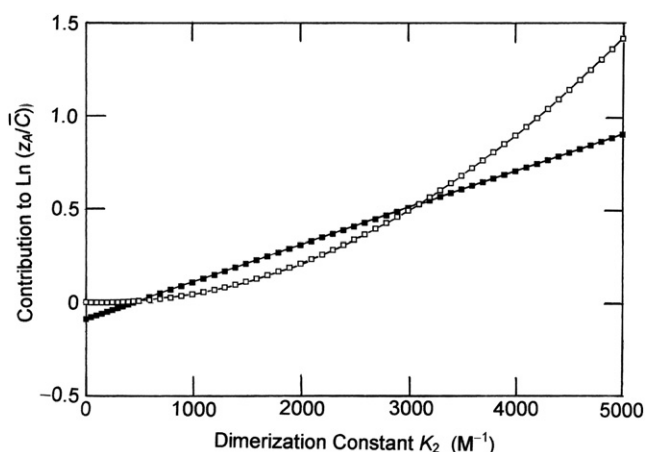


FIGURE 1 Comparison of the contributions of the linear (\blacksquare) and quadratic (\square) concentration terms in the expression for $\ln(z_A/\bar{C})$ with $\bar{C} = 0.1 \text{ mM}$ and a range of dimerization constants. Data are calculated from Eq. 8 with $B_{AA} = 450 \text{ L mol}^{-1}$, $B_{AP} = 1300 \text{ L mol}^{-1}$, and $B_{AAA} = 127,300 \text{ L}^2 \text{ mol}^{-2}$ (see text).

where P is an additional curve-fitting coefficient for a cubic term that has been included to take some account of contributions from higher-order terms—a step taken to improve the reliability of the value deduced for the coefficient of the quadratic term in monomer activity.

The above considerations of a self-associating system in terms of theory for a single solute have led to quantitative expressions that afford relatively simple procedures for the characterization of protein dimerization, provided that a magnitude can be assigned to the second virial coefficient for nonassociative monomer-monomer interaction ($B_2 M_A$ via B_{AA}). However, the absence of quantitative expressions for many of the third and higher-order nonassociative virial coefficients (B_{AAP}, B_{APP} , etc.) restricts this approach to the characterization of dimer and possibly trimer formation (5,6). Other procedures are therefore required to characterize two-state self-association ($nA \rightleftharpoons P$) involving higher oligomeric species.

Thermodynamic nonideality in a two-solute system

The alternative approach is to regard solute self-association as a two-solute system and to consider thermodynamic nonideality as a separate phenomenon, an option that affords a means of making allowance for nonideality arising from nearest-neighbor interactions between monomer (A) and polymer (P) species, irrespective of the size of the latter ($n \geq 2$). However, for illustrative purposes we shall again focus attention on a monomer-dimer association equilibrium in numerical examples to allow readier comparison of this approach with its predecessor. In this more commonly adopted method the thermodynamic activity of each species (z_i) is expressed as the product of its molar concentration (C_i) and an activity coefficient (γ_i), whereupon the relationship between the thermodynamic association constant (K_n) and its apparent value (K_n^{app}), the corresponding ratio of molar concentrations, becomes

$$K_n = \frac{z_P}{z_A^n} = \frac{C_P \gamma_P}{(C_A \gamma_A)^n} = K_n^{\text{app}} \left(\frac{\gamma_P}{\gamma_A^n} \right). \quad (10)$$

Meaningful evaluation of K_n (or $X_n = nK_n/M_A$) is thus dependent upon an ability to assign the appropriate magnitude to the activity coefficient ratio (γ_P/γ_A^n), an endeavor that may be accomplished rigorously by describing activity coefficients on the statistical-mechanical basis of excluded volume (22). However, inspection of those expressions for the two activity coefficients, namely

$$\gamma_A(r) = \exp\left(2\left(\frac{B_{AA}}{M_A}\right)c_A(r) + \left(\frac{B_{AP}}{M_P}\right)c_P(r)\right), \quad (11a)$$

$$\gamma_P(r) = \exp\left(2\left(\frac{B_{PP}}{M_P}\right)c_P(r) + \left(\frac{B_{AP}}{M_A}\right)c_A(r)\right), \quad (11b)$$

reveals two undesirable but still achievable aspects of this approach.

The first obvious drawback is that magnitudes must be assigned not only to B_{AA} but also to the corresponding second virial coefficients for monomer-polymer (B_{AP}) and polymer-polymer (B_{PP}) interactions. On the grounds that the counterparts of Eq. 7 for these two second virial coefficients are

$$B_{AP} = \frac{4\pi L(R_A + R_P)^3}{3} + \frac{Z_A Z_P (1 + \kappa R_A + \kappa R_P)}{2I(1 + \kappa R_A)(1 + \kappa R_P)}, \quad (12a)$$

$$B_{PP} = \frac{16\pi L R_P^3}{3} + \frac{Z_P^2 (1 + 2\kappa R_P)}{4I(1 + \kappa R_P)^2}, \quad (12b)$$

this extra requirement for magnitudes of $\gamma_A(r)$ and $\gamma_P(r)$ can also be met with a reasonable degree of precision by combining measurements of the Stokes radius and net charge of monomer with the concepts of spherical geometry, $R_P = n^{1/3}R_A$, and charge conservation, $Z_P = nZ_A$ (3,4).

The second disconcerting aspect of the approach is its requirement for knowledge of the composition of the solution [$c_A(r)$, $c_P(r)$], which is the information being sought from the experiment. In other words, evaluation of the activity coefficients of the two species is predicated on knowledge of $c_A(r)$ for any given $\bar{c}(r)$, and hence on the adoption of an iterative approach with an initial estimate of the composition deduced from the sedimentation equilibrium distribution on the basis of thermodynamic ideality. Thus, the first fitting of the distribution according to its theoretical description, namely

$$\bar{c}(r) = \frac{M_{AZ_A}(r_F)\psi_A(r)}{\gamma_A(r)} + \frac{X_n(M_{AZ_A}(r_F)\psi_A(r))^n}{\gamma_P(r)}, \quad (13)$$

is conducted with values of unity for the activity coefficients to obtain an initial estimate of $M_{AZ_A}(r_F)$ and hence $M_{AZ_A}(r)$ throughout the distribution via Eq. 4. Substitution of the consequent values of $M_{AZ_A}(r)$ for $c_A(r)$ and $[\bar{c}(r) - c_A(r)]$ for $c_P(r)$ into Eqs. 11a and 11b then provides initial estimates

of $\gamma_A(r)$ and $\gamma_P(r)$ throughout the sedimentation equilibrium distribution. Nonlinear regression of the revised data set [$\psi_A(r), \bar{c}(r), \gamma_A(r), \gamma_P(r)$] in terms of Eq. 13 then leads to improved estimates of $M_{AZ_A}(r_F)$, and hence $c_A(r) = M_{AZ_A}(r_F)\psi_A(r)/\gamma_A(r)$, thereby allowing refinement of the composition and hence activity coefficients. This iterative process is continued until no further change occurs in the returned value of $M_{AZ_A}(r_F)$, whereupon the value of X_n returned as the other curve-fitting parameter is taken as the thermodynamic association constant for reversible dimerization of the solute.

Despite its feasibility, there have only been two applications of this rigorous two-state approach (3,4), which was even abandoned by those authors in favor of developing the simpler single-solute analyses (5,7) already described above. However, the method is revived later in this investigation on the grounds that it affords the sole means of making realistic allowance for effects of nonideality in systems involving two-state self-association beyond dimer.

Excluded volume considerations in terms of scaled particle theory

Scaled particle theory is an alternative statistical mechanical treatment of solution thermodynamic nonideality in terms of excluded volume for uncharged solutes (23,24). Although it has not been used previously for direct analysis of sedimentation equilibrium distributions, scaled particle theory has been adapted to allow for effects of thermodynamic nonideality on the concentration dependence of weight-average molecular mass of self-associating solutes (8–11). Since the use of scaled particle theory for self-associating systems also entails the use of composition-dependent activity coefficients, the direct fitting of sedimentation equilibrium distributions is again possible via the above iterative application of Eq. 13 with values of unity as the initial estimates of γ_A and γ_P . Improved estimates of the two activity coefficients can then be obtained from the equations (8,25)

$$Q\gamma_A(r) = \exp \left[\frac{1}{Q} \cdot \frac{V_A}{M_A} \left(7c_A + \left(\frac{3}{\sqrt[3]{n}} + \frac{3}{\sqrt[3]{n^2}} + \frac{1}{n} \right) (\bar{c}(r) - c_A(r)) \right) + \frac{3}{Q^2} \left(\frac{V_A}{M_A} \right)^2 \left(c_A + \frac{\bar{c}(r) - c_A(r)}{\sqrt[3]{n}} \right) \left(\frac{5}{2} c_A(r) + \left(\frac{3}{2} \sqrt[3]{n} + \frac{1}{\sqrt[3]{n^2}} \right) (\bar{c}(r) - c_A(r)) \right) + \frac{3}{Q^3} \left(c_A + \frac{1}{\sqrt[3]{n}} (\bar{c}(r) - c_A(r)) \right)^3 \right], \quad (14a)$$

$$Q\gamma_P(r) = \exp \left[\frac{1}{Q} \cdot \frac{V_A}{M_A} \left(7x^3 (\bar{c}(r) - c_A(r)) + \left(3\sqrt[3]{nx} + 3\sqrt[3]{n^2}x^2 + nx^3 \right) c_A(r) \right) + \frac{3}{Q^2} \left(\frac{V_A}{M_A} \right)^2 \left(x^3 (\bar{c}(r) - c_A(r)) + \sqrt[3]{n}xc_A(r) \right) \left(\frac{5}{2} x^3 (\bar{c}(r) - c_A(r)) + \left(\frac{3}{2} \sqrt[3]{nx} + \sqrt[3]{n^2}x^2 \right) c_A(r) \right) + \frac{3}{Q^3} \left(\frac{V_A}{M_A} \right)^3 \left(x^3 (\bar{c}(r) - c_A(r)) + \sqrt[3]{n}xc_A(r) \right)^3 \right], \quad (14b)$$

where

$$Q = 1 - \frac{V_A}{M_A} (c_A + x^3(\bar{c}(r) - c_A(r))), \quad (14c)$$

which are rearranged forms of the expressions in Eq. A3 of Chatelier and Minton (8) with $V_A = 4\pi LR_A^3/3$ representing the molar volume of monomer and that of polymer expressed as nx^3V_A : x is unity for the present systems with monomer and polymer modeled as uncharged impenetrable spheres. In keeping with the above approach, the iterative application of Eqs. 13 and 14a–14c clearly has potential for evaluating K_n and $z_A(r_F)$. Indeed, Eqs. 14a and 14b are merely more complicated counterparts of Eqs. 11a and 11b for the activity coefficients.

The Adams-Fujita approach

The original method developed to allow for effects of thermodynamic nonideality in sedimentation equilibrium distributions for reversibly associating solutes (1) is a hybrid of the two-solute and single-solute approaches. Although thermodynamic nonideality is described in terms of an activity coefficient for each species, the single-solute concept is also invoked in the specified dependence of those activity coefficients upon total solute concentration (Eq. 1 above). Inspection of Eqs. 6 and 7 of the investigation describing the NONLIN software (12) shows its reliance upon the same assumptions; and the Beckman Origin software (14) follows the same protocol. As noted above, the main advantage of an activity coefficient approach is its ability to incorporate allowance for the effects of nearest-neighbor nonassociative interactions into the analysis of sedimentation equilibrium distributions reflecting self-association beyond dimer. After incorporating the consequent activity coefficient interrelationship, namely

$$\ln \gamma_P = n \ln \gamma_A \quad (15)$$

and adopting the experimental preference for the weight-concentration scale, the counterpart of Eq. 13 for two-state self-association becomes

$$\bar{c}(r) = \frac{M_A z_A(r_F) \psi_A(r)}{\gamma_A(r)} + X_n \left(\frac{M_A z_A(r_F) \psi_A(r)}{\gamma_A(r)} \right)^n, \quad (16)$$

which clearly has no ready general analytical solution. After substituting the Adams and Fujita interrelationship (1) between activity coefficients (Eq. 1), this expression becomes

$$\begin{aligned} \bar{c}(r) = & (M_A z_A(r_F) \psi_A(r) \exp(-BM_A \bar{c}(r))) \\ & + X_n (M_A z_A(r_F) \psi_A(r) \exp(-BM_A \bar{c}(r)))^n. \end{aligned} \quad (17)$$

Although general solution of Eq. 17 is still not possible because of the incomplete separation of variables, it is amenable to analytical solution for a specified value of BM_A by regarding $\psi_A(r) \exp\{-BM_A \bar{c}(r)\}$ as the independent variable. Subject to adequacy of the Adams and Fujita (1) assumption about composition dependence of activity coefficients for the monomer and oligomer species, analyses of the dependence of $\bar{c}(r)$ upon $\psi_A(r) \exp\{-BM_A \bar{c}(r)\}$ for a range of BM_A values has potential as a means of identifying the most appropriate value of BM_A and hence the best description in terms of curve-fitting parameters, $M_A z_A(r_F)$ and X_n (for a given value of n), on the basis of the goodness-of-fit of the data to Eq. 17.

An alternative approach for a monomer-dimer system ($n = 2$) is to regard Eq. 17 as a quadratic in $\psi_A(r)$ with solution

$$\psi_A(r) = \frac{-1 + [1 + 4X_2 \bar{c}(r)]^{1/2}}{2X_2 z_A(r_F) \exp[BM_A \bar{c}(r)]}. \quad (18)$$

This expression is also amenable to solution for a specified value of BM_A by regarding $\psi_A(r)$ and $\bar{c}(r)$ as the dependent and independent variables, respectively. Although $\bar{c}(r)$ is usually considered to be a function of radius [or $\psi_A(r)$], such reversal of roles for the two experimental variables finds precedent in the INVEQ approach to characterizing solute self-association by sedimentation equilibrium (15) as well as in the application of Eq. 6 (7). Nonlinear least-squares curve-fitting of a $[\bar{c}(r), \psi_A(r)]$ data set to Eq. 18 for a range of BM_A values thus also has potential as a means of determining the dimerization constant as the value of X_2 that emanates from analysis of the data set using the value of BM_A commensurate with the best-fit description (smallest sum of squares of residuals).

METHODS

In this investigation, the task of examining the effectiveness of the various quantitative expressions from the previous section has been simplified by restricting their application to simulated distributions for an uncharged dimerizing solute ($n = 2, Z_A = Z_P = 0$). Initially we examine earlier simulated distributions (7) for such systems involving a 70 kDa monomer with $\bar{v}_p = 0.74$ subjected to sedimentation equilibrium at 293 K and a rotor speed of 7000 rev./min. Specifically, those simulations (7) entailed the assignment of a value of 4.000 L/g to the thermodynamic activity of monomer, $M_A z_A(r_F)$, at a reference radial distance r_F of 7.000 cm in a liquid column spanning the radial distance 6.850–7.150 cm to allow the calculation of $M_A z_A(r)$ as $M_A z_A(r_F) \psi_A(r)$ at 0.002 cm intervals in r (see Eq. 4). The radial dependence of the total weight-concentration of solute, $\bar{c}(r)$, at each radial distance was then calculated from the expression

$$\begin{aligned} \bar{c}(r) = & M_A z_A(r) + \frac{2}{M_A} (K_2 - B_{AA}) (M_A z_A(r))^2 - \frac{3}{M_A^3} \left(K_2 B_{AP} - 2 B_{AA}^2 + \frac{B_{AAA}}{2} \right) (M_A z_A(r))^3 \\ & - \frac{4}{M_A^3} \left(K_2^2 B_{PP} - K_2 \left(2B_{AA} B_{AP} + \frac{B_{AP}^2}{2} \right) - 3B_{AA} B_{AAA} + \left(16 B_{AA}^3 + \frac{B_{AAAA}}{3} \right) \right) (M_A z_A(r))^4, \end{aligned} \quad (19)$$

with values of 450 M^{-1} for B_{AA} , 900 M^{-1} for B_{PP} , 1300 M^{-1} for B_{AP} , $127,000 \text{ M}^{-2}$ for B_{AAA} , $26,370,000 \text{ M}^{-3}$ for B_{AAAA} , and chosen dimerization constants in the range $100 \leq K_2 \leq 1800 \text{ M}^{-1}$. Magnitudes of the virial coefficients are based on respective radii of 3.55 nm and 4.47 nm for monomer and dimer ($R_P = 2^{1/2}R_A$) and Eqs. 4a–4e of the previous nonideality investigation (7). Finally, the simulated concentration distributions were converted to Rayleigh interference counterparts based on 3.33 fringes for 1 mg/mL protein (26), after which a random error of 0.02 fringes, typical of experimental data (15), was superimposed on the fringe distribution. Although allowance for thermodynamic nonideality is only being contemplated at the level of the effects of nearest-neighbor interactions (the quadratic term in concentration), extension of the series in Eq. 18 to the quartic term in monomer activity was required to ensure the simulation of sedimentation equilibrium distributions with a precision greater than the nominal uncertainty (0.02 fringe) applied to each simulated distribution.

The same model solute was used in a second set of simulated low-speed (27) sedimentation experiments in which the monomer activity, $M_A z_A(r_F)$, at the reference radial position (7.000 cm) was decreased to 2.000 g/L and the rotor speed increased to 11,000 rev./min. These changes were made to improve the potential reliability of analyses because of the wider concentration span across the resulting distributions. For example, $\bar{c}(r)$ ranged between 2.6 and 5.7 g/L in simulated distributions for the weakest dimerizing system ($K_2 = 100 \text{ M}^{-1}$) at the lower rotor speed, whereas the corresponding limits were 0.7 and 5.4 g/L in the simulated distribution at 11,000 rev./min (Fig. 2).

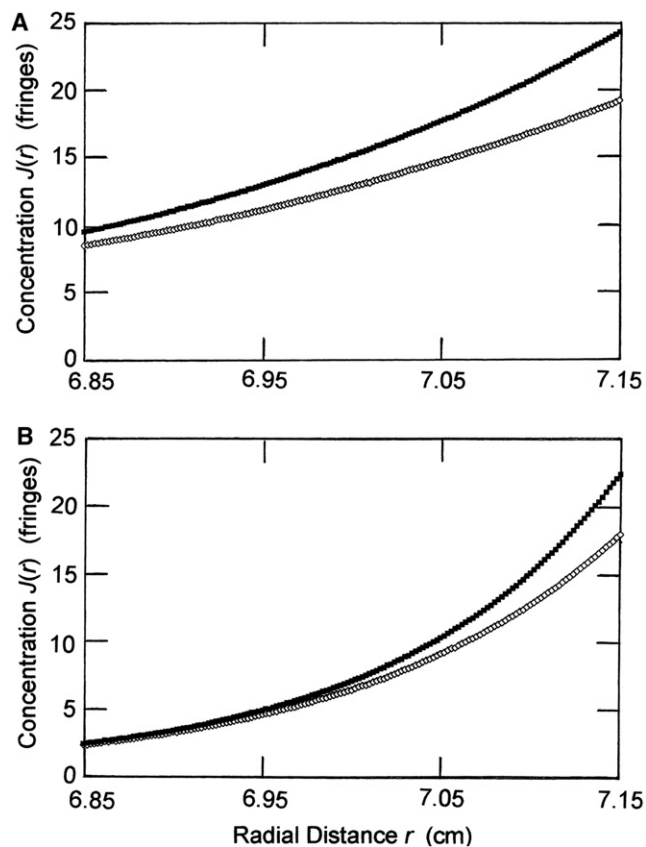


FIGURE 2 Simulated sedimentation equilibrium distributions for a 70 kDa protein undergoing reversible dimerization governed by association constants of 100 M^{-1} (\diamond) and 1800 M^{-1} (\blacksquare), the extremes of the range covered. (A) Rayleigh fringe distributions obtained via Eqs. 9b and 19 with $r_F = 7.000 \text{ cm}$, $M_A z_A(r_F) = 4.000 \text{ g/L}$ and a rotor speed of 7000 rev./min. (B) Corresponding distributions calculated with $M_A z_A(r_F) = 2.000 \text{ g/L}$ and a rotor speed of 11,000 rev./min.

Distributions with even greater concentration spans were then generated by increases of the rotor speed to 15,000, 18,000, and 21,000 rev./min and concomitant decreases in the magnitude of $M_A z_A(r_F)$ to maintain an experimentally measurable concentration [$\bar{c}(r) < 10 \text{ g/L}$ at the cell base]. The form of these distributions approached but did not conform with sedimentation equilibrium distributions of meniscus-depletion design (28) in that $\bar{c}(r)$ at the air-liquid meniscus could not be taken as effectively zero. Nevertheless, distributions such as those generated by these simulations are still amenable to reliable experimental delineation by incorporating a synthetic boundary run into the design of the sedimentation equilibrium investigation (29–31).

Although it is obviously possible to write software to effect analytical solution of the various quantitative expressions developed for the analysis of sedimentation equilibrium distributions reflecting solute dimerization, a manual approach has been adopted in this investigation to provide reader assessment of the consequences of adopting a particular approach on the resulting characterization. Activity coefficients pertaining to each concentration $\bar{c}(r)$ throughout a distribution were therefore obtained by means of an Excel spreadsheet and then pasted into the SCIENTIST package (Micromath Scientific Software, Salt Lake City, UT) for nonlinear least-squares curve-fitting to the appropriate quantitative expression for determination of the best-fit values of K_2 and $M_A z_A(r_F)$.

RESULTS AND DISCUSSION

A major objective of the above theoretical section has been to provide analytical expressions that facilitate critical appraisal of the reliability of incorporating the Adams and Fujita (1) assumption, Eq. 1, into the analysis of sedimentation equilibrium distributions reflecting solute self-association. In that regard it should be noted that Eq. 17 affords an analytical alternative to the NONLIN approach (12,14), whereas Eq. 18 is an analytical counterpart of INVEQ (15). Because the reliability of association constants obtained by these two software packages is the object of current concern, it is appropriate to begin analysis of the simulated sedimentation equilibrium distributions with the application of Eqs. 17 and 18.

Analyses of low-speed distributions based on the Adams-Fujita assumption

In keeping with the NONLIN and INVEQ approaches, the evaluation of a dimerization constant by means of Eqs. 17 and 18 is conditional upon identification of the empirical BM_A coefficient as the value corresponding to a minimum in the sum of squares of residuals (SSR) associated with the best-fit description obtained for each assigned magnitude to BM_A . In that regard, analysis based on Eq. 17 (the analytical counterpart of NONLIN) has met with only limited success inasmuch as no minimum in SSR could be found for half of the 26 low-speed sedimentation equilibrium distributions subjected to scrutiny. Only for distributions reflecting $K_2 \geq 900 \text{ M}^{-1}$ (i.e., $K_2 \geq 2B_{AA}$) was there consistent return of a physically acceptable characterization (a positive dimerization constant and BM_A in reasonable proximity to 0.0129 L/g , the value of $2B_{AA}/M_A$). Greater success in the identification of a value for the Adams-Fujita parameter was achieved by analysis according to Eq. 18 (the counterpart of INVEQ), there

being only one distribution (that for the weakest associating system with $K_2 = 100 \text{ M}^{-1}$ run at the lower speed) for which the SSR increased monotonically with increasing magnitude of the assigned BM_A . However, an input dimerization constant of 800 M^{-1} or greater was required for the consistent return of acceptable K_2 values. Results of both analyses for simulated systems with $800 \leq K_2 \leq 1800 \text{ M}^{-1}$ are summarized in Table S1.

At first glance, the above observations seemingly support the use of Eq. 18 rather than Eq. 17 for characterizing solute dimerization by sedimentation equilibrium. However, closer inspection of Table S1 reveals a consistent disparity between the favored values of BM_A and hence K_2 estimates for systems to which both analyses yield acceptable solutions. This quandary about the appropriate magnitude of BM_A , which should be a function of the protein system rather than the method of analysis, is explored further in Fig. 3 A, which summarizes the two dependencies upon BM_A of the

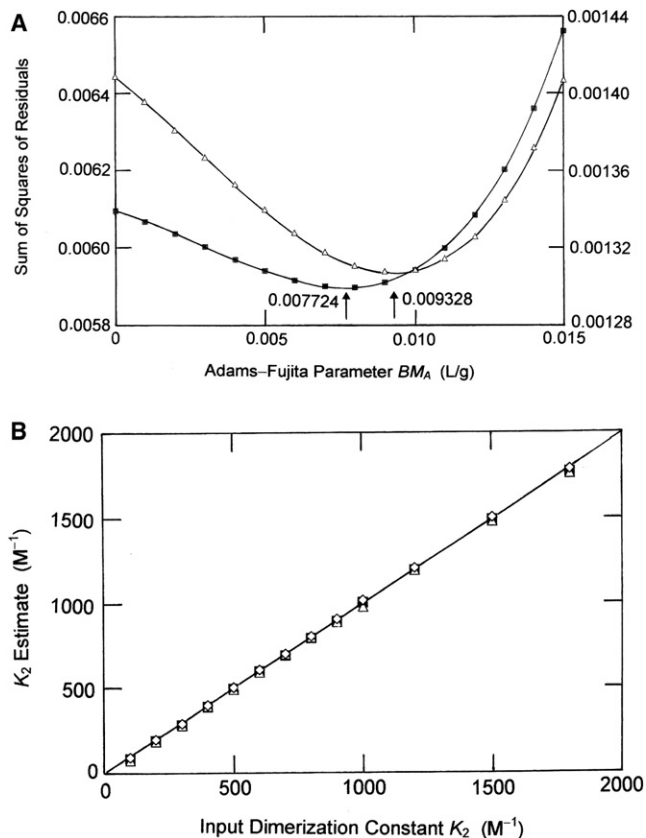


FIGURE 3 (A) Disparity between values of the Adams-Fujita parameter BM_A deduced from the minimum in the sum of squares of residuals (SSR) in nonlinear least-squares curve-fitting of simulated distributions to Eqs. 17 (■, left-hand ordinate) and 18 (△, right-hand ordinate) for the monomer-dimer system with $K_2 = 800 \text{ M}^{-1}$ centrifuged at 11,000 rev./min. (B) Extent of correlation between input dimerization constants and values obtained by curve-fitting simulated sedimentation equilibrium distributions to Eq. 9 (■) as well as by the iterative application of Eq. 13 with activity coefficients determined by means of Eqs. 11a and 11b (△) and 14a–14c (◇). The solid line is the theoretical dependence with a slope of unity.

sum of squares of residuals emanating from nonlinear least-squares curve-fitting of the sedimentation equilibrium distribution simulated at 11,000 rev./min (run B) for the system with $K_2 = 800 \text{ M}^{-1}$. Identification of the appropriate magnitude of BM_A from the position of the minimum in SSR clearly leads to a larger value of the Adams-Fujita parameter from analysis in terms of Eq. 18, this being a systematic feature of all results reported in Table S1. Another point to be noted from Fig. 3 A is the deviation of the dependencies from a symmetrical parabolic relationship, an indication that the model used to determine the fit is incorrect (32).

In the instances where the application of Eq. 17 to sedimentation equilibrium distributions has yielded an acceptable solution, the estimate of K_2 is lower than the value used for the simulation. Indeed, the correlation coefficient ($\pm 2 \text{ SD}$) relating the estimate to the actual value for the set is 0.87 (± 0.04). Although analyses based on Eq. 18 yielded a closer correspondence between K_2 estimates and the input values (a correlation coefficient of 0.92 (± 0.05)), that observation is clouded to some extent by the reversal of roles for the dependent and independent variables employed in such analyses.

Statistical-mechanical approaches

Of the rigorous statistical-mechanical approaches to the analysis of sedimentation equilibrium distributions reflecting reversible nonideal dimerization, the most direct entails nonlinear least-squares curve-fitting of the $[r, \bar{c}(r)]$ data set(s) to Eq. 9, which arises from considerations of self-association as a form of nonideality (5). As noted above, the cubic term (with P a curve-fitting constant) is included to accommodate effects of higher-order virial terms, which would otherwise influence the estimate of the coefficient for the quadratic term in monomer activity—the parameter of prime interest from the viewpoint of determining K_2 (7). In view of the great similarity between Eqs. 9 and 19, the application of this approach to distributions simulated by means of the latter necessarily yields good estimates of $(X_2 - 2B_{AA}/M_A)$ and hence, $K_2 = X_2 M_A / 2$ upon the assignment (via Eq. 7) of the correct magnitude (450 L/mol) to B_{AA} . Indeed, the extent of correlation between estimated and input dimerization constants for the 26 sedimentation equilibrium distributions is $1.003 (\pm 0.011)$.

From Fig. 3 B it is evident that good correlation, 0.996 (± 0.004), is also observed for dimerization constants obtained by the two-state statistical-mechanical approaches involving composition-dependent activity coefficients (Eq. 13 with activity coefficients given either by Eqs. 11a and 11b or by Eqs. 14a–14c). That both statistical mechanical approaches yield essentially identical activity coefficients is confirmed in Table S2. Evaluation of K_2 via Eqs. 11a and 11b does, of course, require the assignment of magnitudes to B_{AP} and B_{PP} (via Eqs. 12a and 12b) as well as to B_{AA} (via Eq. 7), the only requirement for the application of Eq. 9. However, for

an uncharged system these three parameters are all merely functions of monomer radius (R_A), which is also entailed in the specification of (V_A) for the determination of activity coefficients via scaled particle theory (Eqs. 14a–14c with $x = 1$). The advantage of these statistical-mechanical approaches incorporating composition-dependent activity coefficients is their ability to encompass the characterization of two-state self-association involving an oligomer larger than dimer. In this study the four iterations required to achieve solution of Eq. 13 in conjunction with Eqs. 11a and 11b were accomplished within 10–15 min by means of an Excel spreadsheet and the SCIENTIST curve-fitting program (longer times for activity coefficients calculated from scaled particle theory because of the greater complexity of Eqs. 14a–14c). If required, the whole procedure could readily be incorporated into a software package for automation of otherwise tedious calculations.

Analyses of higher-speed distributions

The relatively poor outcomes of analyses based on the Adams-Fujita assumption could, to some extent, reflect the relatively small concentration ranges covered in the simulated low-speed sedimentation equilibrium experiments; but it should be noted that those ranges proved adequate for satisfactory quantitative characterization of solute dimerization by the statistical-mechanical approaches. We now apply the Adams-Fujita analyses (Eqs. 17 and 18) to simulated distributions with an upper concentration limit of 7–10 g/L and a lower limit approaching zero. These distributions from simulated higher-speed sedimentation equilibrium experiments (15,000, 18,000, and 21,000 rev./min) thus span the concentration range over which the restriction of nonideality considerations to effects to nearest-neighbor interactions can reasonably be expected to provide adequate allowance for departures from thermodynamic ideality.

Results from these analyses of higher-speed sedimentation equilibrium distributions for self-associating systems with $600 \leq K_2 \leq 1800 \text{ M}^{-1}$ exhibit better agreement between returned and input values of the dimerization constant than was observed in Table S1. Specifically, the correlation is $0.945 (\pm 0.025)$ for analysis according to Eq. 17, and $0.962 (\pm 0.024)$ for analysis via Eq. 18 (data not shown). However, the inability of either analysis to establish reliable values of BM_A and hence, dimerization constant persists for systems with $K_2 \leq 500 \text{ M}^{-1}$. Insight into the likely source of this deficiency comes from Fig. 4, which presents the dependencies of the sums-of-squares of residuals upon the magnitude of the Adams-Fujita parameter BM_A to which the best-fit description of simulated distributions at 15,000 rev./min refers. Incompatibility with analysis in terms of the Adams-Fujita approach is shown by systems with $K_2 < 300 \text{ M}^{-1}$, for which the SSR increases monotonically with BM_A . As K_2 approaches B_{AA} (450 L/mol), the form of the dependence changes in that the dependence of the sum-of-squares of residuals upon BM_A

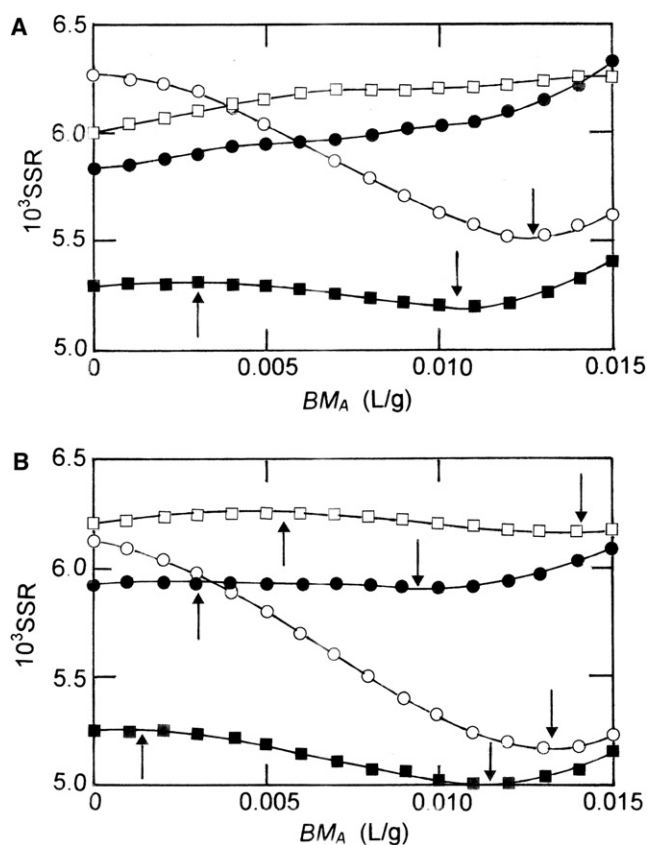


FIGURE 4 Dependence of the sums-of-squares of residuals associated with best-fit descriptions of the equilibrium distributions simulated sedimentation at 15,000 rev./min of reversibly self-associating systems involving a 70 kDa monomer and dimerization constants of 300 M^{-1} (\square), 400 M^{-1} (\bullet), 500 M^{-1} (\blacksquare), and 600 M^{-1} (\circ). (A) Analyses according to Eq. 17; (B) Analysis via Eq. 18. Arrows indicate the positions of maxima (\uparrow) and minima (\downarrow) in the dependencies.

exhibits a maximum (as well as the predicted minimum in some cases) for systems with dimerization constants of $300\text{--}500 \text{ M}^{-1}$, an effect more pronounced in analysis via the INVEQ analog (Fig. 4). However, the overall variation in SSR with BM_A is sufficiently small to render questionable the reliability of assigning significance to the value of BM_A associated with the low-point of such shallow minima: only for the system with $K_2 = 600 \text{ M}^{-1}$ does the depth of the minimum suffice to engender much confidence in its precise location. Further increases of K_2 beyond B_{AA} leads to residuals plots with more clearly defined minima, a feature that allows greater confidence to be placed on use of the consequent value of BM_A for the determination of K_2 by the Adams-Fujita approach. This consideration has dictated the setting of a lower limit of 600 M^{-1} for K_2 in further considerations.

The fact that physically acceptable magnitudes were invariably returned for BM_A and X_2 in analyses of each of the simulated higher-speed distributions according to Eqs. 17 and 18 signifies their seeming conformity with the Adams-Fujita assumption. Accordingly, the three distributions were

subjected to a global analysis by identifying r_F (see Eq. 9b) as the radial distance in each distribution corresponding to a common concentration, $\bar{c}(r_F)$, of 3.00 g/L (i.e., $J(r_F) = 10.00$ fringes) to allow their analysis in terms of a single value of $M_A Z_A(r_F)$. Results for the simulated systems with $600 \leq K_2 \leq 1800 \text{ M}^{-1}$ are summarized in columns 2 and 3 of Table 1, about which the following points are noted.

1. Although the dependence of the sum-of-squares of residuals upon BM_A for the system with $K_2 = 600 \text{ M}^{-1}$ analyzed according to Eq. 17 exhibited a minimum for the individual data sets, the difference between the locations of those minima sufficed to generate a combined dependence exhibiting a monotonic increase of SSR with BM_A and hence, a situation in which K_2 could not be evaluated.
2. As noted in relation to Table S1, the values of K_2 deduced by applying Eq. 18 are consistently slightly higher than those emanating from analysis according to Eq. 17.
3. The uncertainties in the K_2 values obtained by curve-fitting to the different models afford little insight into the likely accuracy of the estimate, a situation that was encountered previously in an application of global curve-fitting of sedimentation equilibrium distributions for the ovalbumin-cytochrome *c* system (33).
4. Although the returned values of K_2 may be regarded as acceptable estimates of the input dimerization constants (correlation coefficients of $0.94 (\pm 0.04)$ and $0.96 (\pm 0.03)$ for the respective analyses according to Eqs. 17 and 18), analysis by the statistical-mechanical approaches is superior in that regard—a point illustrated by the inclusion of results from global curve-fitting according to Eqs. 9a and 9b (column 4), for which the correlation coefficient is $1.00 (\pm 0.01)$.
5. Despite the theoretical deficiencies of the Adams-Fujita assumption (1), its use should not influence adversely the analysis of high-speed sedimentation equilibrium distributions for dimerizing systems with $K_2 > B_{AA}$ ($X_2 > BM_A$). For systems in which the contribution of thermo-

dynamic nonideality outweighs that of self-association, ($K_2 \leq B_{AA}$), the statistical-mechanical approaches provide the only reliable means of analysis.

Analysis of distributions via NONLIN

As noted in the Introduction, the NONLIN (12) and Beckman Origin (14) software packages as well as the published version of the INVEQ (15) algorithm all incorporate the Adams-Fujita assumption (1), Eq. 1, to allow for effects of thermodynamic nonideality in the characterization of solute self-association by sedimentation equilibrium. On the grounds that analytical solution of the basic quantitative expressions incorporating the Adams-Fujita assumption (Eqs. 17 and 18) has signified limitations of the approach for weakly dimerizing systems ($K_2 \leq B_{AA}$), it seems highly probable that a similar deficiency will pervade analyses via software employing algorithms to effect solution of the same basic quantitative expressions. That inductive logic has been confirmed by applying the NONLIN software to the higher-speed sedimentation equilibrium distributions for which analysis via Eqs. 17 and 18 has already been described (Table 1).

Attempts to characterize the dimerization by NONLIN analysis (12) of the simulated distributions for the weakest systems were unsuccessful in that no self-association was detected for systems with $K_2 \leq 300 \text{ M}^{-1}$, the returned estimate being extremely small with an upper limiting value (100- to 100,000-fold larger). These findings undoubtedly reflect inability of the program to locate the appropriate values of BM_A because, as already seen from analyses according to Eqs. 17 and 18, they cannot be identified based on a minimum in the sum-of-squares of residuals. Of greater concern are the low estimates of K_2 returned for the systems with the higher dimerization constants that were amenable to evaluation by the application of Eqs. 17 and 18 (column 5 of Table 1). Indeed, it is debatable whether this use of NONLIN has led to any better characterization than that (column 6 of Table 1) based on assumed thermodynamic ideality ($\gamma_A = \gamma_P$ in Eq. 17). To what extent the low results reflect the automatic

TABLE 1 Summary of best-fit estimates of the dimerization constant K_2 obtained by global analysis of simulated sedimentation equilibrium distributions at 15,000, 18,000, and 21,000 rev./min

Input K_2 (M^{-1})	Evaluated dimerization constant (M^{-1})				
	Eq. 17*	Eq. 18*	Eq. 9*	NONLIN [†]	$\gamma_A = \gamma_P = 1^*$
600	NV [‡]	572 (± 11)	600 (± 38)	202 (166–244)	61 (± 8)
700	742 (± 8)	750 (± 8)	725 (± 27)	253 (214–302)	137 (± 6)
800	806 (± 8)	822 (± 8)	821 (± 29)	268 (228–315)	216 (± 7)
900	750 (± 9)	803 (± 10)	881 (± 35)	255 (217–303)	287 (± 8)
1000	906 (± 9)	938 (± 10)	997 (± 34)	301 (255–351)	364 (± 8)
1200	1154 (± 10)	1178 (± 10)	1218 (± 34)	351 (303–405)	513 (± 9)
1500	1391 (± 10)	1396 (± 11)	1495 (± 33)	443 (387–504)	734 (± 9)
1800	1705 (± 11)	1719 (± 12)	1805 (± 38)	531 (472–594)	933 (± 12)

Simulations refer to a 70 kDa monomer with $R_A = 3.55 \text{ nm}$, $R_P = 4.47 \text{ nm}$.

*Numbers in parentheses denote twice the standard deviation of the estimate.

[†]Ranges denoted limits based on a 65% probability (12).

[‡]No minimum observed in the sum of squares of residuals.

incorporation of baseline corrections has not been ascertained: for the systems we are using in this article, that baseline correction should have been zero because the concentrations distributions subjected to analysis contained no systematic error. Our decision to refrain from interfering with the NONLIN program is justified on the grounds that a baseline correction is inevitably going to be applied in its routine analysis of any experimental Rayleigh fringe distribution.

CONCLUDING REMARKS

This investigation into the use of sedimentation equilibrium for the quantitative characterization of nonideal solute self-association by sedimentation equilibrium has served several important roles.

Firstly, from a theoretical viewpoint, an important outcome is the deduction of analytical solutions (Eqs. 17 and 18) to the quantitative expression for radial variation of total solute concentration that incorporates a widely accepted assumption about the composition-dependence of species activity coefficients (1).

Secondly, it has highlighted the failure of Eq. 1, the widely accepted expression (1) for the concentration dependence of activity coefficients, to describe adequately the consequences that stem from considerations of thermodynamic nonideality on the statistical-mechanical basis of excluded volume (22) for weakly associating systems ($K_2 \leq B_{AA}$). In that regard, the findings in this article amplify the much earlier observations (2) that prompted the development of other approaches for the characterization of solute self-association by sedimentation equilibrium (3–11,17,18,33). Nevertheless, provided that the experimental sedimentation equilibrium distributions examined cover the concentration range 0–10 g/L, adoption of the Adams-Fujita assumption (1) still leads to an acceptable quantitative characterization of systems characterized by higher dimerization constants (Table 1); but its adoption for the analysis of low-speed (27) sedimentation equilibrium distributions is of questionable value (Table S1). This is, in fact, an important and extremely fortunate outcome for users of the Adams-Fujita assumption, because curve-fitting is being used to evaluate a parameter that is actually a composition-dependent variable (2).

Thirdly, a matter of great concern has been our failure to obtain adequate quantitative descriptions of the simulated distributions by the application of NONLIN, a software package (12) that solves the same expression for the radial dependence of solute concentration by means of algorithms and simulation. Furthermore, similar problems are likely to be encountered with the Beckman Origin (14) software package and the published INVEQ algorithm (15) because of their reliance on similar simulative and algorithmic ploys to extract the dimerization constant.

Fourthly, two analytical approaches incorporating allowance for thermodynamic nonideality on the statistical-mechanical basis of excluded volume have been shown to yield

acceptable descriptions of simulated sedimentation equilibrium distributions for an uncharged solute system (Fig. 3 B). Although analysis in terms of Eq. 9 provides the simpler means of characterizing solute dimerization, the iterative application of Eq. 13 has the advantage of rendering possible the characterization of solute self-association involving an oligomer greater than dimer.

Finally, this demonstration of the inability of the Adams-Fujita approach to accommodate the characterization of weak self-association renders highly desirable the replacement of current software packages by computer programs, incorporating the statistical-mechanical approaches, to allow for effects of thermodynamic nonideality in sedimentation equilibrium distributions reflecting solute self-association.

SUPPORTING MATERIAL

Two tables are available at [http://www.biophysj.org/biophysj/supplemental/S0006-3495\(09\)01034-0](http://www.biophysj.org/biophysj/supplemental/S0006-3495(09)01034-0).

REFERENCES

- Adams, E. T., and H. Fujita. 1963. Sedimentation equilibrium in interacting systems. *In* Ultracentrifugal Analysis in Theory and Experiment. J. W. Williams, editor. Academic Press, New York.
- Ogston, A. G., and D. J. Winzor. 1975. Treatment of thermodynamic non-ideality in equilibrium studies of associating solutes. *J. Phys. Chem.* 79:2496–2500.
- Wills, P. R., L. W. Nichol, and R. J. Siezen. 1980. The indefinite self-association of lysozyme: consideration of composition-dependent activity coefficients. *Biophys. Chem.* 11:71–82.
- Jacobsen, M. P., and D. J. Winzor. 1992. Refinement of the omega analysis for the quantitative characterization of solute self-association by sedimentation equilibrium. *Biophys. Chem.* 45:119–132.
- Wills, P. R., M. P. Jacobsen, and D. J. Winzor. 1996. Direct analysis of solute self-association by sedimentation equilibrium. *Biopolymers.* 38:119–130.
- Wills, P. R., and D. J. Winzor. 2001. Studies of solute self-association by sedimentation equilibrium: allowance for effects of thermodynamic non-ideality beyond the consequences of nearest-neighbor interactions. *Biophys. Chem.* 91:253–262.
- Winzor, D. J., and P. R. Wills. 2007. Characterization of weak protein self-association by direct analysis of sedimentation equilibrium distributions: the INVEQ approach. *Anal. Biochem.* 368:168–177.
- Chatelier, R. C., and A. P. Minton. 1987. Sedimentation equilibrium in macromolecular solutions of arbitrary concentration. 1. Self-associating proteins. *Biopolymers.* 26:507–524.
- Muramatsu, N., and A. P. Minton. 1989. Hidden self-association of proteins. *J. Mol. Recognit.* 1:166–171.
- Zorilla, S., M. Jiménez, P. Lillo, G. Rivas, and A. P. Minton. 2004. Sedimentation equilibrium in a solution containing an arbitrary number of solute species at arbitrary concentrations: theory and application to concentrated solutions of ribonuclease. *Biophys. Chem.* 108: 89–100.
- Jiménez, M., G. Rivas, and A. P. Minton. 2007. Quantitative characterization of weak self-association in concentrated solutions of immunoglobulin G via the measurement of sedimentation equilibrium and osmotic pressure. *Biochemistry.* 46:8373–8378.
- Johnson, M. L., J. J. Correia, D. A. Yphantis, and H. R. Halvorson. 1981. Analysis of data from analytical ultracentrifugation by nonlinear least-squares techniques. *Biophys. J.* 36:575–588.

13. Milthorpe, B. K., P. D. Jeffrey, and L. W. Nichol. 1975. Direct analysis of sedimentation equilibrium results obtained with polymerizing systems. *Biophys. Chem.* 3:169–175.
14. McRorie, D. K., and P. J. Voelker. 1993. Self-Associating Systems in the Analytical Ultracentrifuge. Beckman Instruments, Palo Alto, CA.
15. Rowe, A. J. 2005. Weak interactions: optical algorithms for their study in the AUC. In *Modern Analytical Ultracentrifugation: Techniques and Methods*. D. J. Scott, S. E. Harding, and A. J. Rowe, editors. Royal Society of Chemistry, Cambridge, UK.
16. Hill, T. L., and Y. D. Chen. 1973. Theory of aggregation in solution. 1. General equations and application to the stacking of bases, nucleosides, etc. *Biopolymers*. 12:1285–1312.
17. Wills, P. R., and D. J. Winzor. 1992. Thermodynamic non-ideality and sedimentation equilibrium. In *Analytical Ultracentrifugation in Biochemistry and Polymer Science*. S. E. Harding, A. J. Rowe, and J. C. Horton, editors. Royal Society of Chemistry, Cambridge, UK.
18. Wills, P. R., and D. J. Winzor. 2005. Allowance for thermodynamic non-ideality in sedimentation equilibrium. In *Modern Analytical Ultracentrifugation: Techniques and Methods*. D. J. Scott, S. E. Harding, and A. J. Rowe, editors. Royal Society of Chemistry, Cambridge, UK.
19. Haschemeyer, R. H., and W. F. Bowers. 1970. Exponential analysis of concentration or concentration difference data for discrete molecular weight distributions in sedimentation equilibrium. *Biochemistry*. 9:435–445.
20. Wills, P. R., W. D. Comper, and D. J. Winzor. 1993. Thermodynamic non-ideality in macromolecular solutions: interpretation of virial coefficients. *Arch. Biochem. Biophys.* 300:206–212.
21. Winzor, D. J., and P. R. Wills. 1994. The omega analysis and the characterization of solute self-association by sedimentation equilibrium. In *Modern Analytical Ultracentrifugation: Acquisition and Interpretation of Data*. T. M. Schuster and T. M. Laue, editors. Birkhäuser, Boston, MA.
22. McMillan, W. G., and J. E. Mayer. 1945. The statistical thermodynamics of multicomponent systems. *J. Chem. Phys.* 13:276–305.
23. Reiss, H., H. L. Frisch, and J. L. Lebowitz. 1959. Statistical mechanics of rigid spheres. *J. Chem. Phys.* 31:369–380.
24. Lebowitz, J. L., E. Helfand, and E. Praestgaard. 1965. Scaled particle theory of fluid mixtures. *J. Chem. Phys.* 43:774–779.
25. Gibbons, R. M. 1969. The scaled particle theory for particles of arbitrary shape. *Mol. Phys.* 17:81–86.
26. Voelker, P. 1995. Measurement of the extinction coefficient of prostate specific antigen using interference and absorbance optics in the Optima XL-A analytical ultracentrifuge. *Prog. Colloid Polym. Sci.* 99:162–166.
27. Van Holde, K. E., and R. L. Baldwin. 1958. Rapid attainment of sedimentation equilibrium. *J. Phys. Chem.* 62:734–743.
28. Yphantis, D. A. 1964. Equilibrium centrifugation in dilute solutions. *Biochemistry*. 3:297–317.
29. Richards, E. G., and H. K. Schachman. 1959. Ultracentrifuge studies with Rayleigh interference optics. I. General application. *J. Phys. Chem.* 63:1578–1591.
30. Richards, E. G., D. C. Teller, and H. K. Schachman. 1968. Ultracentrifuge studies with Rayleigh interference optics. II. Low-speed sedimentation equilibrium of homogeneous systems. *Biochemistry*. 7:1054–1076.
31. Hall, D. R., S. E. Harding, and D. J. Winzor. 1999. The correct analysis of low-speed sedimentation equilibrium distributions recorded by the Rayleigh interference optical system in a Beckman XL-I ultracentrifuge. *Prog. Colloid Polym. Sci.* 113:62–68.
32. Brooks, I., D. G. Watts, K. K. Sonesson, and P. Hensley. 1994. Determining confidence intervals for parameters derived from analysis of equilibrium analytical ultracentrifugation data. *Methods Enzymol.* 240:458–459.
33. Wills, P. R., M. P. Jacobsen, and D. J. Winzor. 2000. Analysis of sedimentation equilibrium distributions reflecting non-ideal macromolecular associations. *Biophys. J.* 79:2178–2187.